metals

MDPI

Article

Optimization of Quenching and Tempering Parameters for the Precipitation of M_7C_3 and MC Secondary Carbides and the Removal of the Austenite Retained in Vanadis 10 Tool Steel

Alejandro Gonzalez-Pociño, Florentino Alvarez-Antolin * and Juan Asensio-Lozano

Materials Pro Group, Departamento de Ciencia de los Materiales e Ingeniería Metalúrgica, Universidad de Oviedo, Independencia 13, 33004 Oviedo, Spain; UO204622@uniovi.es (A.G.-P.); jasensio@uniovi.es (J.A.-L.)

* Correspondence: alvarezflorentino@uniovi.es; Tel.: +34-985-181-9491

Received: 2 May 2019; Accepted: 27 May 2019; Published: 29 May 2019

Abstract: Vanadis 10 steel is a powder metallurgy processed tool steel. The aim of the present study is to analyze the microstructural variation in this steel that takes place when the process variables related to the heat treatments of quenching and tempering are modified. Specifically, the destabilization of austenite, the precipitation of secondary carbides and the amount of retained austenite were analyzed. The research methodology employed was a Design of Experiments (DoE). The percentage and types of precipitated crystalline phases were determined by XRD, while the microstructure was revealed by means of SEM-energy-dispersive X-ray spectroscopy (EDX). The destabilization of austenite was favored by tempering at 600 °C for at least 4 h. These same conditions stimulated the removal of the retained austenite and the precipitation of M_7C_3 secondary carbides. For the precipitation of MC secondary carbides, it was necessary to maintain the steel at a temperature of 1100 °C for at least 8 h. The highest hardness values were obtained when the tempering temperature was lower (500 °C). Tempering in air or oil did not have a significant influence on the hardness of the steel after double or triple tempering at 500 or 600 °C. These results allow the manufacturers of industrial tools and components that use this type of steel in the annealed state as a material to define the most suitable quenching and tempering heat treatment to optimize the in-service behavior of these steels.

Keywords: high speed steel; powder metallurgy; retained austenite; secondary carbides; X-ray diffraction; hardness

1. Introduction

Tool steels for cold work are used in the manufacture of tooling used to form materials. These steels require a specific set of properties such as high hardness and wear resistance, so their carbon contents are high. They are also required to have a tough in-service performance [1]. The presence of carbide-forming elements such as Cr, Mo, W and V achieve an enhancement in both quenchability and wear resistance [2].

The end of solidification of these steels gives rise to a ledeburitic eutectic. When these steels are manufactured via conventional casting, they present a high degree of dendritic segregation, a heterogeneous microstructure and a continuous network of large carbides. These characteristics result in low toughness and high anisotropy in the steels' mechanical properties. To eliminate this dendritic segregation, it is necessary to perform a homogenization annealing, while a hot forging process is required to fragment and disperse the carbide network. During the process of manufacturing industrial components from these steels, machining is needed. To facilitate their machining, these steels need to

be subjected to a softening annealing. The final properties required for the material can subsequently be obtained via quenching and tempering [3]. The manufacture of these steels by powder metallurgy (PM) enables the elimination of the dendritic segregation, obtaining more homogeneous properties in the entire piece and the uniform, dispersed distribution of carbides [4].

Their microstructure is mainly made up of M_7C_3 carbides, associated with Cr, and of the MC type, associated with V. M_7C_3 carbides, precipitated as a consequence of the reduction in the solubility limit of the austenite phase, are fully dissolved in the austenite at a temperature of 1100 °C. However, MC carbides are "lazier" and dissolve to a lesser extent. The dissolution of Cr and part of the V allows an increase in the hardness of the material after being quenched in oil [5,6]. Nevertheless, wear resistance may be improved by promoting the destabilization of austenite in the 1000–1100 °C temperature range [7]. As a result of this destabilization of the austenite, chromium-rich secondary carbides, mainly of the M_7C_3 type, precipitate [8–10]. To achieve this, dwell times of longer than 4 h are required at the austenitization temperature [8]. The destabilization of austenite will increase the Ms temperature, reducing the risk of fracture during quenching and decreasing the percentage of retained austenite [11]. In steels of this type, tempering has a very significant influence on the amount of retained austenite [12]. During tempering, secondary hardening may occur due to the precipitation of M_7C_3 [13] and MC carbides [14–16]. This would occur if, after the destabilization of austenite, carbide-forming elements remained dissolved in it. During subsequent tempering at temperatures of around 600 °C, a fine dispersion of nanometric carbides could precipitate on the martensite [17]. A double or triple tempering would enable a large part of the retained austenite to be transformed into martensite [18]. The transformation of the retained austenite during tempering takes place at temperatures below 470 °C [19]. A sub-zero treatment between the austenitization treatment and the tempering would enable the removal of the retained austenite [20].

Vanadis 10 steel is a ledeburitic steel processed by powder metallurgy (PM) marketed by the UDDEHOLM company (Hagfors, Sweden). Its main alloying elements are V (around 10%) and Cr (around 8%). The aim of the present study is to analyze the microstructural variation that Vanadis 10 steel undergoes when the process variables related to the heat treatments of quenching and tempering are modified. Specifically, the destabilization of austenite, the precipitation of secondary carbides and the amount of retained austenite are analyzed. All these microstructural variations are correlated with the hardness of the material.

2. Materials and Methods

Table 1 shows Vanadis 10 steel's chemical composition. Its high percentages of C, Cr and V are worth noting. Its microstructure in the annealed state is formed by a ferritic matrix with two types of uniformly distributed carbides, M_7C_3 and MC [21].

Table 1. Chemical composition (wt.%).

C	Si	Mn	Cr	Mo	V
2.9	0.5	0.5	8	1.5	9.8

The purpose of applying the Design of Experiments (DoE) statistical technique was to modify certain working conditions deliberately so as to produce changes in one or more of the responses under study. For example, the working conditions of five factors linked to quenching and tempering conditions were modified in this study. The aim was to analyze the effect of these variations on the microstructure and hardness of the material. Table 2 shows the factors and values that these factors should take so as to vary the working conditions in an orderly manner. In this case, six factors were analyzed, with two levels for each factor. If the DoE were factorial, the experiment would be carried out with all possible combinations of factors and levels. That is, it would be necessary to execute a total of 2^5 (32) experiments. The effect of a factor is the variation in the response function as a

consequence of the variation of said factor. These effects are defined as the main effects. In most cases, the effect of one factor depends on the value that another takes. When this occurs, these factors are said to interact. The influence of the main effects on a particular response is greater than that of the interactions of two factors, while the influence of the latter is in turn greater than that of the interactions of three factors, and so on. In practice, it is extremely rare for interactions of three or more factors to appear that are found to be significant. That is, sufficiently approximate models are obtained considering only the main effects and the two-factor interactions, thus allowing us to reduce the number of experiments. In this case, eight experiments were carried out, so we only estimate eight effects (2^{5-2}), which supposes a one-fourth (32/8) fractional factorial design. This means that three other effects are confounded in each effect. Table 3 shows the resulting array of experiments. The set of generators associated with this array of experiments is D = AB and E = AC [22]. That is, columns D and E were respectively constructed from the product of columns A × B and A × C. The "Confounding Pattern" column indicates those second-order interactions whose effects are confounded with the main effects. The confounding pattern should include all the effects confounded with each other. However, Table 3 shows a restricted confounding pattern in which only the main effects and the two-factor interactions are represented.

Each main effect may be considered a random variable where the obtained value is an estimate of its mean. The effects are linear combinations of the analyzed responses and, applying the Central Limit Theorem, will accordingly follow a normal distribution. If all the effects were non-significant, they would follow an N(0,σ) law and would thus appear aligned in a representation of the effects on a normal probability plot. If any effect is significant, however, it will follow an N(μ,σ) law, not appearing aligned with the non-significant effects. Those effects that deviate from the straight line towards the ends on the normal probability plot are significant [22]. Those that deviate to the left indicate that the value of the response increases at their −1 level, while those that deviate to the right indicate that the value of the response increases at their +1 level.

Table 2. Factors and levels.

Factors			Levels	
Code	**Description of the Factors**	**Unit**	**−1 Level**	**+1 Level**
A	Tempering temperature	°C	500	600
B	Dwell time at 1100 °C	h	4	8
C	Quench cooling medium	-	air	oil
D	Number of temperings	-	2	3
E	Tempering time	h	2	4

Table 3. Array of experiments.

No.	A	B	C	D	E	Restricted Confounding Pattern
1	−1	−1	−1	+1	+1	A+BD+CE B+AD C+AE D+AB E+AC BC+DE BE+CD
2	+1	−1	−1	−1	−1	
3	−1	+1	−1	−1	+1	
4	+1	+1	−1	+1	−1	
5	−1	−1	+1	+1	−1	
6	+1	−1	+1	−1	+1	
7	−1	+1	+1	−1	−1	
8	+1	+1	+1	+1	+1	

The analyzed responses were:

- The Vickers hardness—the applied load was of 1000 N, while the value of hardness considered in each experiment was the average value obtained from 10 indentations;
- Microstructural variables, such as the percentage of carbides and the amount of martensite present.

Nital 4% (4 mL nitric acid and 96 mL ethanol) was used as an etching solution to reveal the microstructure of the material following mechanical grinding and polishing. The optical microscope employed was a NIKON Epiphot 200 (Nikon, Tokyo, Japan), and images were obtained using the Omnimet Enterprise Image Analysis System. The different types of precipitated carbides were identified under a JEOL JSM-5600 scanning electron microscope (SEM, JEOL, Nieuw-Vennep, The Netherlands) equipped with the characteristic X-ray scattering microanalysis system (SEM-energy-dispersive X-ray spectroscopy (EDX)).

The percentages and types of co-existing crystalline phases were determined by X-ray diffraction (XRD, Baker Hughes, Celle, Germany), employing Cu as the emitting metal. The diffractometer used for this purpose was a PANalyticalX'Pert Pro MPD belonging to the University of Oviedo Scientific-Technical Services. The Rietveld structural refinement method was used to identify the percentages of the crystalline phases. To do so, starting with the recording of the diffraction figures, a structural refinement was carried out using the crystallographic information files present in the ICSD inorganic structures database (version 2016, FIZ Karlsruhe, Eggenstein-Leopoldshafen, Germany) belonging to the phases that, according to the technical literature, may be precipitated after the different heat treatments. From the position of the Bragg peaks, the Rietveld structural refinement algorithm allows the adjustment of the dimensions of the crystalline cell.

3. Results

Figure 1 shows a representative micrograph of the Vanadis 10 steel in the annealed state. Its microstructure is made up of ferrite forming the matrix and a high density of carbides, whose diameters are around 1–3 μm.

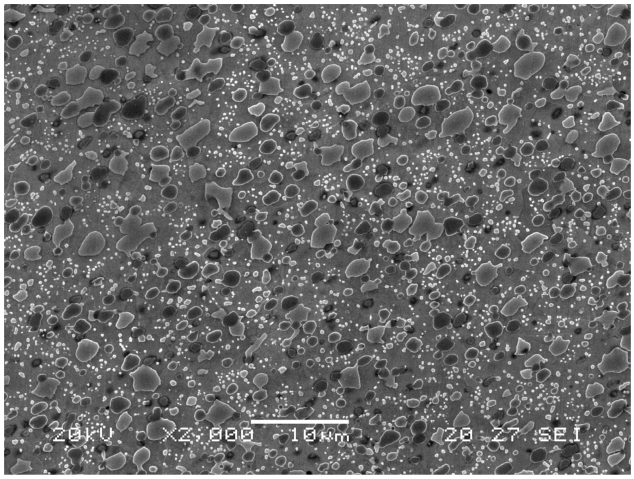

Figure 1. Micrograph of the Vanadis 10 steel in the annealed state. Image was obtained by scanning electron microscope (SEM).

Figure 2 shows the diffractograms for the eight experiments, obtained by X-ray diffraction (XRD). Figure 3 shows the adjustment using Rietveld structural refinement method. Table 4 shows the weight percentages and the lattice parameters of the main crystalline phases detected by XRD in each of the eight experiments. Note that the majority phase in all the experiments is martensite and that the main carbides detected are VC and Cr_7C_3. It should also be noted that the presence of retained austenite was only detected in Experiments 3, 5 and 7.

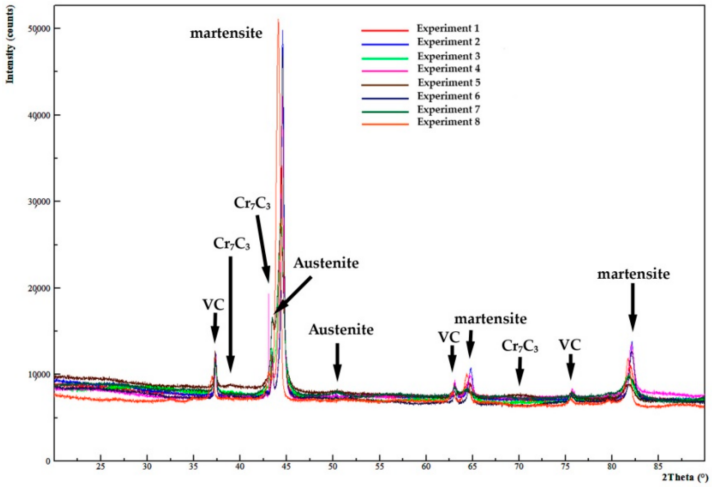

Figure 2. Diffractograms obtained by X-ray diffraction (XRD).

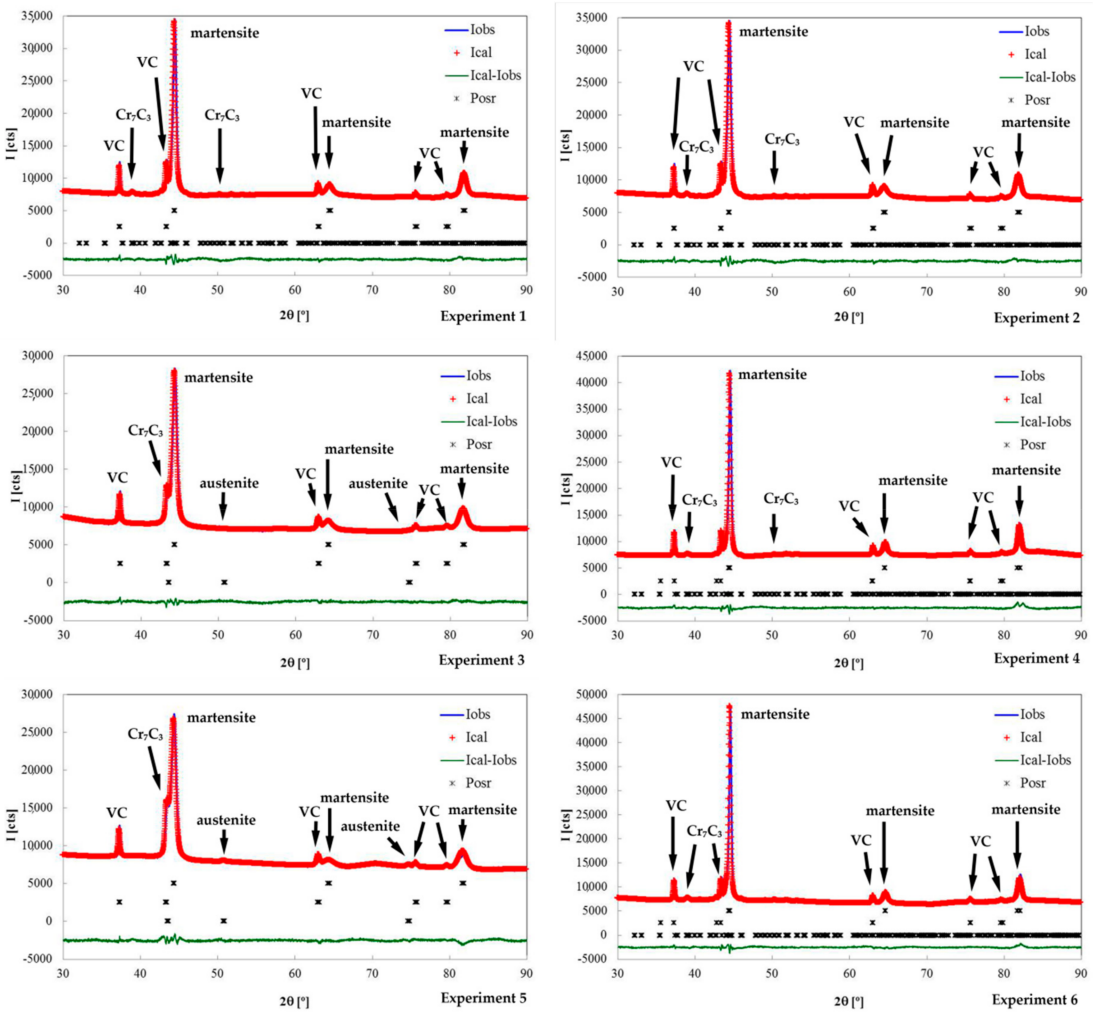

Figure 3. *Cont*.

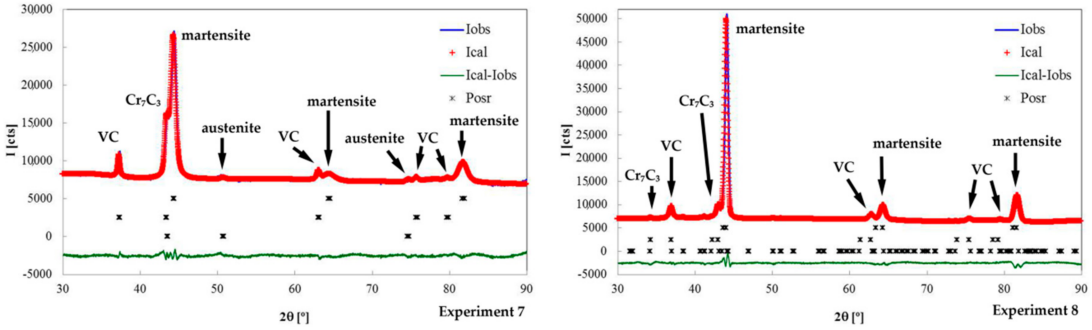

Figure 3. Adjustment using the Rietveld method. The red crosses mark the intensities observed. The blue line shows the intensity calculated according to the structural model. The green line shows the difference between both and the asterisks positions of the different reflections.

Table 4. Microstructural parameters and weight distributions of the precipitated phases. Esd. represents the statistical error.

Experiment	Rietveld Fitting	Phases	a (Å)	b (Å)	c (Å)	wt.%	Esd.
1	Rwp = 9.21 Chi2 = 1.91	Martensite	2.878			76.90	±1.33
		Austenite				-	-
		VC	4.162			15.10	±0.55
		Cr_7C_3	4.504	7.033	12.214	8.00	±1.05
2	Rwp = 9.81 Chi2 = 2.28	Martensite	2.873			74.14	±1.09
		Austenite				-	-
		VC	4.163			15.24	±0.53
		Cr_7C_3	4.504	7.033	12.214	10.62	±0.91
3	Rwp = 8.35 Chi2 = 1.51	Martensite	2.884			78.19	±1.49
		Austenite	3.588			1.46	±0.49
		VC	4.168			18.95	±0.77
		Cr_7C_3	4.504	7.033	12.214	1.40	±0.28
4	Rwp = 10.9 Chi2 = 2.37	Martensite	2.874			76.86	±1.23
		Austenite				-	-
		VC	4.162			15.56	±0.54
		Cr_7C_3	4.504	7.033	12.214	7.58	±0.98
5	Rwp = 10.1 Chi2 = 2.13	Martensite	2.883			69.70	±1.38
		Austenite	3.588			12.56	±0.57
		VC	4.164			15.64	±0.74
		Cr_7C_3	4.504	7.033	12.214	2.10	±0.37
6	Rwp = 9.24 Chi2 = 2.07	Martensite	2.874			74.57	±1.10
		Austenite				-	-
		VC	4.165			14.46	±0.53
		Cr_7C_3	4.504	7.033	12.214	10.97	±0.90
7	Rwp = 10.5 Chi2 = 2.28	Martensite	2.880			71.45	±1.33
		Austenite	3.588			12.08	±0.54
		VC	4.159			14.46	±0.73
		Cr_7C_3	4.504	7.033	12.214	2.01	±0.34
8	Rwp = 10.5 Chi2 = 2.16	Martensite	2.870			75.95	±1.11
		Austenite				-	-
		VC	4.148			19.21	±0.77
		Cr_7C_3	4.504	7.033	12.214	4.84	±0.61

Table 5 shows the mean values obtained in each experiment, together with the effects corresponding to the restricted confounding pattern specified in the array of experiments. The row corresponding to the mean shows the average value obtained for each of the responses. Figure 2 shows the representation

of these standardized effects on a normal probabilistic plot, highlighting those that have a significant effect on these responses.

Table 5. Mean values and effects obtained for the analyzed responses.

(a) Hardness			
Experiment	**HV100**	**Effect**	**Effect**
1	836	673	Average
2	500	−329.5	A+BC+CE
3	825	−11.5	B+AD+CF
4	534	−1.5	C+AE+BF
5	861	10	D+AB+EF
6	518	−16	E+AC+DF
7	829	−23	F+BC+DE
8	481	−12.5	AF+BE+CD

(b) Carbides					
Experiment	**Cr7C3**		**VC**		**Effect**
	(wt.%)	**Effect**	**(wt.%)**	**Effect**	
1	8.00	5.94	15.10	16.08	Average
2	10.62	5.12	15.24	0.08	A+BC+CE
3	1.40	−3.96	18.95	1.93	B+AD+CF
4	7.58	−1.92	15.56	−0.27	C+AE+BF
5	2.10	−0.62	15.64	0.60	D+AB+EF
6	10.97	0.72	14.46	1.70	E+AC+DF
7	2.01	0.85	14.46	−0.15	F+BC+DE
8	4.84	−2.4	19.21	2.36	AF+BE+CD

(c) Retained Austenite			
Experiment	**Austenite**		**Effect**
	(wt.%)	**Effect**	
1	-	3.26	Average
2	-	−6.52	A+BC+CE
3	1.46	0.24	B+AD+CF
4	-	5.79	C+AE+BF
5	12.56	−0.24	D+AB+EF
6	-	−5.79	E+AC+DF
7	12.08	−0.48	F+BC+DE
8	-	0.48	AF+BE+CD

Figure 4a shows that the only factor with a significant effect on hardness is A, the tempering temperature. It also indicates that in order to increase the hardness value, the tempering temperature should be at its −1 level, i.e., at 500 °C.

Figure 4b shows that the only factor that has a significant influence on the percentage of precipitated Cr_7C_3 carbides is Factor A (tempering temperature). Thus, if the aim is to increase the amount of Cr_7C_3 carbides, this factor should be placed at its +1 level (tempering temperature of 600 °C).

Figure 4c shows that the factors that have a significant effect on the percentage of VC are B (dwell time at the austenization temperature) and E (tempering time). Thus, placing these factors at their +1 levels leads to an increase in the percentage of VC. It is also verified that the effect of these factors separately is reinforced if both factors are situated at their aforementioned +1 levels (interaction BE). From this result, it can be deduced that the prolonged dwell times at the destabilization temperature of austenite (8 h at 1100 °C) and the tempering temperature (4 h) are the factors that favor the precipitation of secondary vanadium carbides. However, high tempering temperatures (600 °C) lead to an increase in the precipitation of Cr_7C_3 secondary carbides.

Figure 4d shows that the factors that have a significant effect on the percentage of retained austenite are A (tempering temperature) and E (tempering time). Hence, if the aim is to increase this percentage, both factors should be placed at their +1 levels. That is, tempering should be carried out at 600 °C for 4 h. It is thus verified that prolonged tempering times (4 h) are favorable for the destabilization of austenite and that its transformation into martensite is promoted at a tempering temperature of 600 °C. This result complements the fact that there is an increase in the precipitation of Cr_7C_3 secondary carbides at this tempering temperature. Moreover, it is also observed that interaction AE has a significant effect on the percentage of retained austenite. This means that if both factors are simultaneously placed at their −1 levels, i.e., tempered at 500 °C for 2 h, an increase in retained austenite occurs (see Table 6).

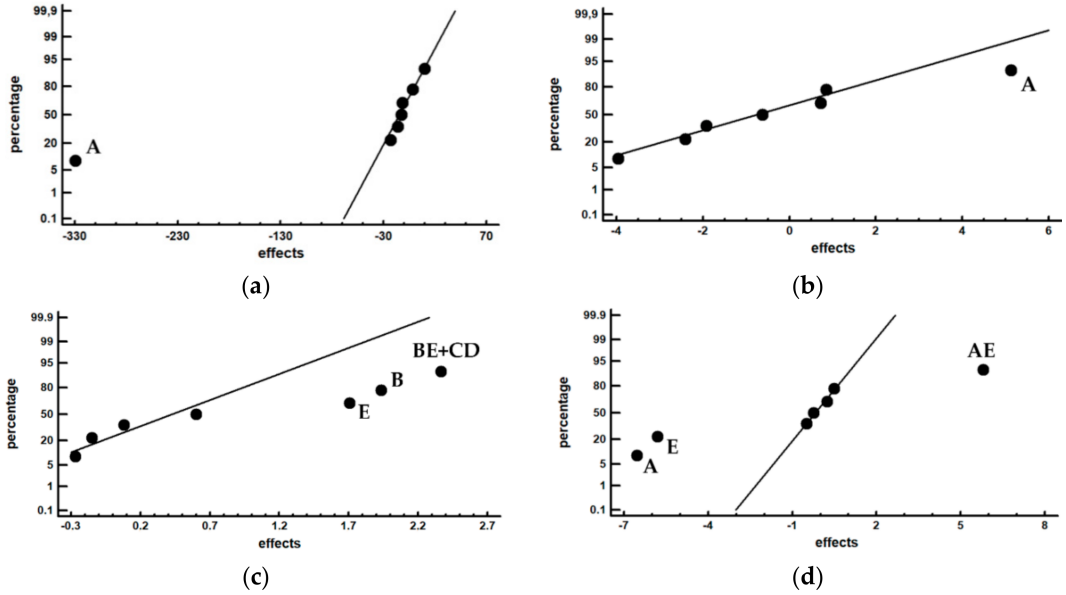

Figure 4. Effects on a normal probability plot. Those factors that have a significant effect on hardness, the percentage of carbides and the percentage of retained austenite are shown. (**a**) Hardness; (**b**) Cr_7C_3 carbides; (**c**) vanadium carbides; (**d**) retained austenite.

Figure 5 shows an example of the microstructure of two samples corresponding to Experiments 2 and 5. Experiment 2 corresponded to a tempering temperature of 600 °C and Experiment 5 to a tempering temperature of 500 °C. The VC and Cr_7C3 carbides are identified by arrows. These carbides were identified from a "mapping" obtained via EDX. This mapping shows the distribution of the elements V and Cr; see Figure 4 for an example. Furthermore, microanalysis via dispersion of energy-dispersive X-ray spectroscopy (EDX) found that these were carbides. It can be seen that the sample in Experiment 2 underwent greater destabilization of austenite during said tempering, as a high density of secondary carbides was observed, which, according to the reddish coloration in the matrix constituent (Figure 6), were mostly of the Cr_7C_3 type. In the sample corresponding to Experiment 2, a particle of Mo_2C was detected, which, due to its scarce presence, was not detected in the XRD analysis when the intensity of its signal was confounded with experimental error. When the contents in Mo are around 1%, the Mo is mainly dissolved in solid solution [23]. Mo_2C carbides can precipitate during tempering within the500–600 °C temperature range [17,24]. Furthermore, the sample corresponding to Experiment 5 showed 12.56% retained austenite. In addition to being tempered at 500 °C, this sample was also subjected to the shortest tempering times (2 h).

Table 6. Analysis of the effect of interaction AE on the retained austenite. It can be seen that placing both factors at their −1 levels leads to a greater increase in retained austenite.

AE	−1	+1
−1	12.3	0.7
+1	0	0

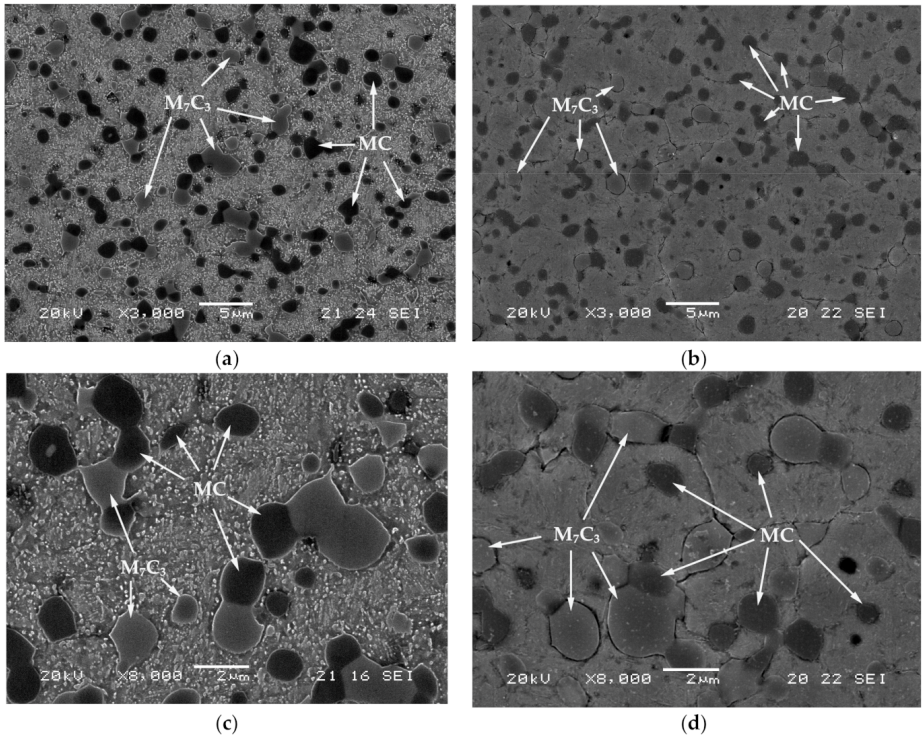

Figure 5. Secondary electron images (SEI) of: (**a**) microstructure corresponding to Experiment 2; (**b**) microstructure corresponding to Experiment 5; (**c**) microstructural details of Experiment 2 observed at a higher magnification; (**d**) microstructural details of Experiment 5 seen at a higher magnification. It can be seen that the sample corresponding to Experiment 2 has a higher density of secondary carbides. Images were obtained by scanning electron microscope (SEM).

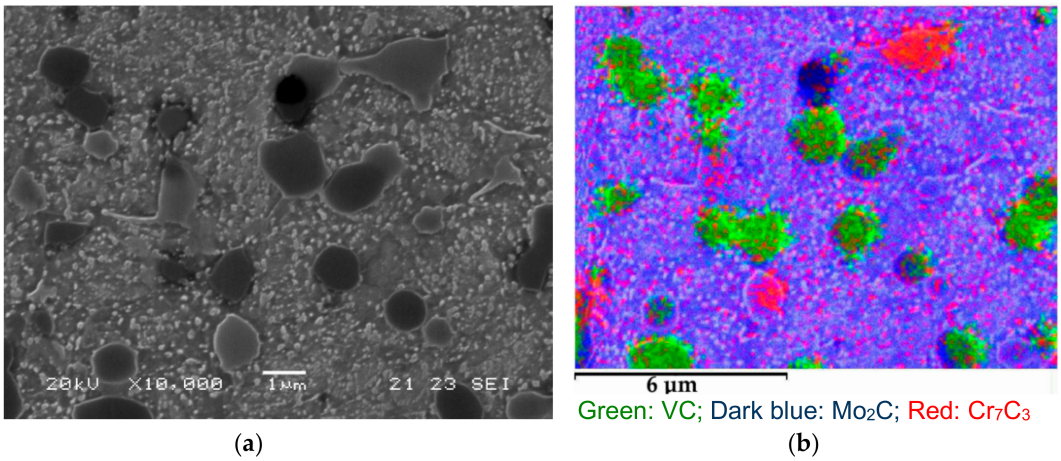

Figure 6. Distribution of carbides in the sample corresponding to Experiment 2. A single particle of Mo_2C can be observed. Based on the reddish coloration in the matrix, it would appear that the majority of the precipitated secondary carbides are of the Cr_7C_3 type. (**a**) Scanning electron microscopy (SEM) image. (**b**) Mapping of elements by means of energy dispersive X-ray (EDX) microanalysis.

4. Conclusions

Regarding the parameters that govern the quenching and tempering processes in Vanadis 10 commercial tool steel, the following is concluded:

1. The destabilization of austenite is favored by high tempering temperatures (600 °C) and prolonged dwell times at this temperature (at least 4 h). These same conditions favor the removal of the retained austenite and the precipitation of Cr_7C_3 secondary carbides.
2. Prolonged dwell times at the destabilization temperature of austenite (at least 8 h at 1100 °C) as well as high dwell times at the tempering temperature (at least 4 h) favor the precipitation of secondary vanadium carbides.
3. However, given that the majority phase is martensite, the higher hardness values are obtained at a tempering temperature as low as 500 °C. The severity of quenching, corresponding to either air or oil, was shown not to have a significant influence on the final hardness value of the steel regardless of double or triple tempering treatment being applied.

Author Contributions: J.A.-L. conceived and designed the experiments; A.G.-P. performed the experiments; F.A.-A. analyzed the data and wrote the paper.

Funding: This research received no external funding.

Conflicts of Interest: The authors declare no conflict of interest.

References

1. Jurci, P. Cr-V Ledeburitic cold-work tool steels. *Materiali in Tehnologije* **2011**, *45*, 383–394.
2. Pippel, E.; Woltersdorf, J.; Pockl, G.; Lichtenegger, G. Microstructure and nanochemistry of carbide precipitates in high-speed steel S 6-5-2-5. *Mater. Charact.* **1999**, *43*, 41–55. [CrossRef]
3. Talacchia, S.; Amador, J.; Urcola, J. High speed tool steel cut off dies made using powder metallurgy techniques. *Revista De Metalurgia* **1996**, *32*, 18–24. [CrossRef]
4. Nemec, M.; Jurci, P.; Kosnacova, P.; Kucerova, M. Evaluation of structural isotropy of Cr-V ledeburitic steel made by powder metallurgy of rapidly solidified particles. *Kovove Materialy Met. Mater.* **2016**, *54*, 453–462. [CrossRef]
5. Bilek, P.; Sobotova, J.; Jurci, P. Evaluation of the microstructural changes in Cr-V ledeburitic tool steels depending on the austenitization temperature. *Materiali in Tehnologije* **2011**, *45*, 489–493.
6. Jurci, P.; Domankova, M.; Ptacinova, J. Evolution of carbide phases in quenched, sub-zero treated and tempered vanadis 6 ledeburitic tool steel. In Proceedings of the Metal 2014: 23rd International Conference on Metallurgy and Materials, Brno, Czech Republic, 21–23 May 2014; pp. 593–599.
7. Gonzalez-Pociño, A.; Alvarez-Antolin, F.; Asensio-Lozano, J. Erosive wear resistance regarding diferent destabilization heat treatments of austenite in high chromium white cast iron, alloyed with Mo. *Metals* **2019**, *9*, 522. [CrossRef]
8. Powell, G.L.F.; Bee, J.V. Secondary carbide precipitation in an 18 wt% Cr-1 wt% Mo white iron. *J. Mater. Sci.* **1996**, *31*, 707–711. [CrossRef]
9. Filipovic, M.M. Iron-chromium-carbon-vanadium white cast irons—The microstructure and properties. *Hemijska Industrija* **2014**, *68*, 413–427. [CrossRef]
10. Guitar, M.A.; Suarez, S.; Prat, O.; Guigou, M.D.; Gari, V.; Pereira, G.; Mucklich, F. High chromium cast irons: destabilized-subcritical secondary carbide precipitation and its effect on hardness and wear properties. *J. Mater. Eng. Perform.* **2018**, *27*, 3877–3885. [CrossRef]
11. Efremenko, V.G.; Chabak, Y.G.; Brykov, M.N. Kinetic parameters of secondary carbide precipitation in high-Cr white iron alloyed by Mn-Ni-Mo-V complex. *J. Mater. Eng. Perform.* **2013**, *22*, 1378–1385. [CrossRef]
12. Hui, L.; Han-Guang, F.; Jiang, J.; Jun, W. Effect of heat treatment on microstructure and property of high vanadium wear-resistant alloy. *Materialwissenschaft Und Werkstofftechnik* **2018**, *49*, 1485–1493. [CrossRef]
13. Durica, J.; Ptacinova, J.; Hudakova, M.; Kusy, M.; Jurci, P. Microstructure and Hardness of cold work vanadis 6 steel after subzero treatment at-140 degrees C. *Adv. Mater. Sci. Eng.* **2018**, 7. [CrossRef]
14. Yan, F.; Shi, H.S.; Fan, J.F.; Xu, Z. An investigation of secondary carbides in the spray-formed high alloyed Vanadis 4 steel during tempering. *Mater. Charact.* **2008**, *59*, 883–889. [CrossRef]

15. Wilmes, S.; Zwick, G. Effecto of niobium and vanadium as an alloying element in toll steels with high chromium content. In Proceedings of the Sixth International Tooling Conference, Karlstad, Sweden, 10–13 September 2002; pp. 269–287.
16. Jurci, P.; Domankova, M.; Hudakova, M.; Ptacinova, J.; Pasak, M.; Palcek, P. Characterization of microstructure and tempering response of conventionally quenched, short- and long-time sub-zero treated PM Vanadis 6 ledeburitic tool steel. *Mater. Charact.* **2017**, *134*, 398–415. [CrossRef]
17. Pero-Sanz, J.A. *Aceros*; Dossat: Madrid, Spain, 2004; p. 558.
18. Vilar, R.; Colaco, R.; Almeida, A. *Laser surface treatment of tool steels. Laser Processing: Surface Treatment and Film Deposition*; Woodhead Publishing: Sawston, UK, 2012; Volume 307, pp. 453–478.
19. Jurci, P.; Domankova, M.; Ptacinova, J.; Pasak, M.; Kusy, M.; Priknerova, P. Investigation of the Microstructural Changes and Hardness Variations of Sub-Zero Treated Cr-V Ledeburitic Tool Steel Due to the Tempering Treatment. *J. Mater. Eng. Perform.* **2018**, *27*, 1514–1529. [CrossRef]
20. Sobotova, J.; Jurci, P.; Dlouhy, I. The effect of subzero treatment on microstructure, fracture toughness, and wear resistance of Vanadis 6 tool steel. *Mater. Sci. Eng.* **2016**, *652*, 192–204. [CrossRef]
21. Jurci, P.; Domankova, M.; Caplovic, L.; Ptacinova, J.; Sobotova, J.; Salabova, P.; Prikner, O.; Sustarsic, B.; Jenko, D. Microstructure and hardness of sub-zero treated and no tempered P/M Vanadis 6 ledeburitic tool steel. *Vacuum* **2015**, *111*, 92–101. [CrossRef]
22. Prat-Bartés, A.; Tort-Martorell, X.; Grima-Cintas, P.; Pozueta-Fernández, L.; Solé-Vidal, I. *MétodosEstadísticos*, 2nd ed.; UPC: Barcelona, Spain, 2004; p. 376.
23. Wei, S.Z.; Zhu, J.H.; Xu, L.J. Effects of vanadium and carbon on microstructures and abrasive wear resistance of high speed steel. *Tribol. Int.* **2006**, *39*, 641–648. [CrossRef]
24. Antolin, J.F.A.; Garrote, L.F.; Lozano, J.A. Application of Rietveld Refinement to the correlation of the microstructure evolution of white cast irons with 18 and 25%-wt. Cr after oil quench and successive temper treatments, with abrasive wear and bending testing. *Revista De Metalurgia* **2018**, *54*, 11. [CrossRef]